AIAA JOURNAL
Vol. 36, No. 3, March 1998

Multidimensional, Magnetohydrodynamic Simulation of Solar-Generated Disturbances: Space Weather Forecasting of Geomagnetic Storms

Murray Dryer*
National Oceanic and Atmospheric Administration, Boulder, Colorado 80303

A short review is given, first, of an extension of classical, continuum gasdynamics to solar system magnetohydrodynamics (MHD) in both the steady and time-dependent contexts. A slightly longer review is given of two- and three-dimensional, numerical, MHD simulations of transient, solar-generated disturbances in the inner solar system. Validation of this approach is provided by making use of several examples wherein shock shapes and energetic particle fluxes (generated by shocks) are empirically confirmed. Although these studies are based on an ideal, one-fluid (proton) plasma, we suggest that a three-dimensional MHD model be employed to make use of presently available solar observations as approximate physical parameters for initialization conditions. Such a model may be useful, within the space weather national implementation plan, for geomagnetic storm forecasts.

I. Introduction

IT has been recognized that "as the world moves into the 21st century, our civilization is relying more and more on technology that is affected in some way by conditions in the space environment."[1] The importance of forecasting space weather several days in advance of a geomagnetic storm has been reviewed by Allen and Wilkinson.[2] Thus, the recently formulated National Space Weather Program (NSWP) has recognized that three-dimensional, numerical, magnetohydrodynamic (MHD) modeling must play a critical role in a seamless forecasting system. This system refers to space weather originating on the sun; propagation of disturbances through the solar wind and interplanetary magnetic field (IMF), and thence, transmission into the magnetosphere, ionosphere, and thermosphere. This role comes as no surprise to fluid dynamicists who have participated in the numerical modeling of flows, at all Mach numbers, around vehicles in a variety of atmospheric environments as well as the meteorological conditions at Earth and other planets.

For example, the numerical solution[3] of the direct blunt body problem has been applied to the flow of the supersonic/super-Alfvénic solar wind around the magnetospheres of Earth[4–6] and the (then unknown) outer planets' magnetospheres.[7,8] The simple, but basic, assumption here is that the solar wind proton gyroradius is small relative to the magnetospheric obstacle's diameter; thus, the continuum approximation (as in classical gasdynamics) is a reasonable approach for the prediction of macroscopic properties of the fully ionized plasma and magnetic fields. What was called the transition region in the aerodynamics community is now called the magnetosheath in the magnetospheric community. Technology transition, thus applied, was confined briefly to the steady-flow application. In fact, it is being applied as part of the NSWP implementation plan for operational use[9] by the U.S. Air Force's 55th Space Weather Squadron (55 SWX) at Falcon Air Force Base, Colorado.

Unsteady gasdynamic flow formulations[10–12] were also applied to astrophysical and solar system applications.[10,13] Much of this work has been reviewed by this writer[14–17] from a perspective that will be obvious to the aerodynamics community, which is very familiar with fluid theory, wind-tunnel testing, and numerical simulations. Part of this work[18–20] is also being implemented by 55 SWX for operational use.

Given this brief introduction, the problem faced by the modeler (who is interested in developing a first-generation three-dimensional MHD model for technology transitioning to operational space weather forecasting) is as follows: 1) operational, real-time solar observations (optical, x ray, radio, etc.) must be used to generate physical parameters to initialize, and to update, background and transient solar wind conditions for a three-dimensional MHD code and 2) spacecraft data at Earth (outside the bow shock) or at the libration point L1 must be used as ground truth to validate the output of the code. The objective here is to provide accurate predictions of the dynamic pressure and the southerly component of the IMF, B_z. These are the two basic physical parameters that affect the magnetosphere's shape and coupling of electrodynamic energy from the solar wind into the magnetosphere.

The purpose of this paper is to demonstrate several validation cases. Several two-dimensional cases, which show the first applications of matching a code's output with multiple spacecraft data for shock shape and particle energization verification, are presented. A three-dimensional case will illustrate an approach for a solar event that did not involve a flare. A second three-dimensional case will consider a more complex situation during March 1991, when a series of major flares took place. Sections II and III will discuss the two- and three-dimensional cases, respectively. Some concluding remarks will be made in Sec. IV.

II. Examples of Two-Dimensional MHD Studies

As implied in the Introduction, the basic challenge to the modeler who wishes to make extended, i.e., several days, forecasts of geomagnetic storms is this: When will the storm start? How intense will it be? How long will it last? The when question is addressed first, followed by a brief illustration of the application of a two-dimensional code's use for predicting shock acceleration of energetic particles.

It is essential to stress an important point. All of the model examples discussed in these multidimensional MHD cases are initiated at $18R_\odot$ ($R_\odot$ is the solar radius, 6.95×10^5 km). This particular starting position was selected because it is located in the supersonic and super-Alfvénic steady-state region where all characteristics are directed into the computational domain. We will limit the outer boundary for the two-dimensional examples to about 1.6 AU. An astronomical unit is equal to 1.5×10^8 km. If the lower boundary were located closer to the sun, where some characteristics would be directed from within the domain back to the lower boundary, undesirable nonphysical reflected characteristics could be present. This is a complicated numerical problem,[21] which has only recently been solved[22–24] for coronal mass ejection (CME) problems[25] initiated at $1R_\odot$. As yet, there has been no seamless coupling of these recent studies to those discussed in this paper, although a preliminary study[26] has been made. This writer can only suggest that consideration of this multiple critical points problem would be a secondary issue as far as practical applications to space weather predictions are concerned.

Received June 3, 1997; presented as Paper 97-2419 at the AIAA 28th Plasmadynamics and Lasers Conference, Atlanta, GA, June 23–25, 1997; accepted for publication Nov. 28, 1997.

*Guest Worker Emeritus, Space Environment Center, Environmental Research Laboratories, 325 Broadway. Associate Fellow AIAA.

As noted in the Introduction, real-time observational data must be used to infer physical initialization parameters [here six (eight) values for the two-dimensional (three-dimensional) components of velocity and magnetic field, density, and temperature]. According to one view, until we improve our basic understanding of solar flares, CMEs, etc., we cannot (in principal) develop and deploy valid models.[1] This writer takes the view that this ideal is too far in the future; thus, we must use the available observations to infer approximations (yes, educated guesses sometimes) for many of these physical values as functions of space and time. Specifically, coronal holes are known to be observed in the line of HeI 1083 nm; thus, heliolatitudinal and heliolongitudinal (θ, ϕ) spatial boundaries can be used for an assumed higher velocity distribution within the hole. Obviously, only ϕ boundaries are needed for the two-dimensional ecliptic plane examples discussed subsequently. A representative, uniform solar wind velocity (or even an empirically determined ambient flow) can be used for the initial state before such a corotating stream (with anticorrelated density to maintain constant momentum flux) is introduced as an initializing condition, keeping all other parameters unchanged at the lower boundary.

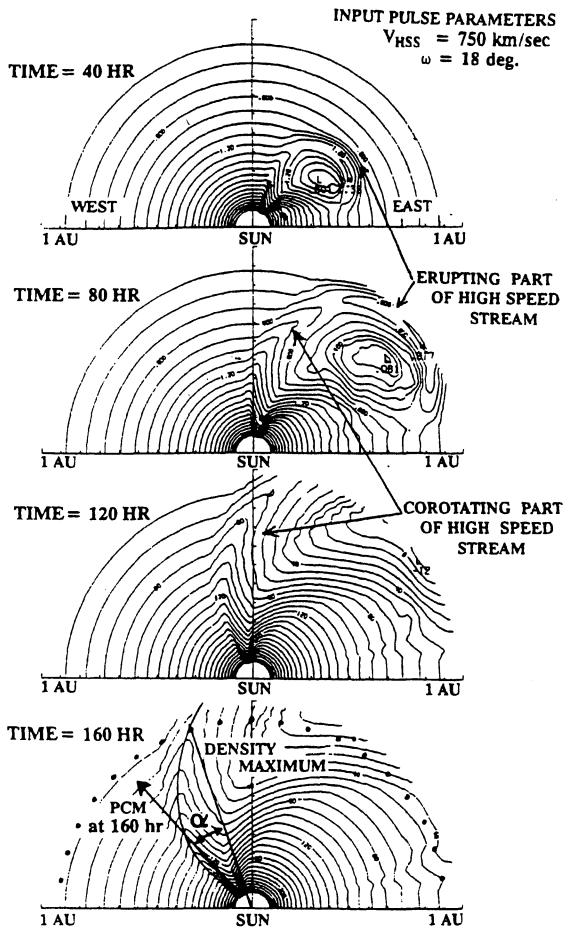

Fig. 1 Evolution of a typical high-speed stream; contours represent solar wind density (from Ref. 27).

To simulate a flare, the location is given by optical observations in the $H\alpha$ line or, alternatively, by soft x-ray images (if available). Also, the U.S. Air Force's (USAF's) Radio Solar Telescope Network provides a shock velocity estimate in the low corona by using a combination of their radio sweep-frequency drift (called a type II radio burst) with time and a model of the coronal electron density as a function of altitude. The exciter mechanism, i.e., the shock, and its velocity are, therefore, found on the physical basis of plasma radio emission at a frequency proportional to the square root of the local coronal density. The shock is then assumed to travel outwardly to and beyond the inner boundary ($18R_\odot$) of the two-dimensional (three-dimensional) simulation's computational domain. The duration of magnetic energy conversion to kinetic, thermal, and potential forms can be approximated by using the proxy soft x-ray flux duration, available in real-time from the National Oceanic and Atmospheric Administration (NOAA) GOES spacecraft. Thus, the blast or piston-driven[10,18] character of the shock can be approximated. The shock velocity, converted to a magnetoacoustic Mach number, will provide a set of peak jump conditions for all variables above the flare site. These initializing conditions may be assumed to be spatially attenuated over an included angle of 60 deg (for example). We discuss applications of this approach to several flare and nonflare examples.

Figure 1 demonstrates a basic two-dimensional solar simulation[27]: transient solar wind response to a newly formed coronal hole's high speed stream, followed by the steady-state corotating low-velocity stream. The peak velocity in the high-speed stream (width $= \omega = 18$ deg $= \Delta\phi$) was assumed to be $V_{HSS} = 750$ km/s. After 160 h, this high-speed stream continuous pulse's central meridian has rotated westward as shown. Displayed in Fig. 1 are solar wind density contours. We will discuss another nonflare example within the three-dimensional context in Sec. III. In this nonflare area, we remark that the Cauchy–Riemann initial boundary value problem will require judicious application of available and continuous observations to deduce reasonable initializing parameters. Figure 2 shows a simulation, again in two dimensions of solar wind transient responses to some of the February 1986 flares[28] that occurred during the last solar minimum. The positions of Earth and four spacecraft are also indicated for validation purposes. The contours are absolute total interplanetary magnetic field $\boldsymbol{B}$. A small degree of iteration (coronal shock velocity, mainly) was necessary to achieve acceptable shock arrival times and data comparisons necessary at Earth (Imp-8), Giotto, Sakigake, Vega-1, and Vega-2. Thus, the feasibility

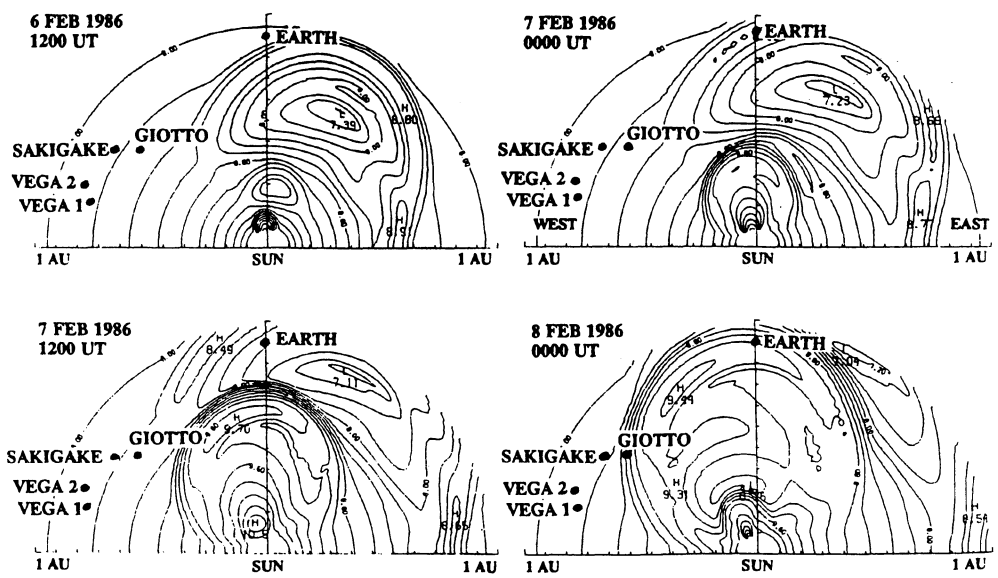

Fig. 2 Simulation of contours of the interplanetary magnetic field B magnitude at four successive times during Feb. 6–8, 1986 (from Ref. 28).

of the MHD deterministic approach for large-scale plasma and magnetic field responses is demonstrated.

The two-dimensional MHD approach was also successful as a vehicle for predicting the anisotropy and flux of 1.6-MeV shock-accelerated protons for east, west, and central meridian events.[29] The sources of these events were both flares and erupting filaments. Figure 3 shows the transient connectivity of the IMF field lines from the expanding shocks to the European Space Agency/European Space Research and Technology Center instrument on ISEE-3. The efficacy of the additional check on the deterministic fluid approach was established by ensuring (iteratively) the shocks' arrivals at Helios-1 and Helios-2, as indicated in Fig. 3.

III. Examples of Three-Dimensional MHD Studies

We are presently investigating the three-dimensional application to the April 14–23, 1994, event that was generated by a southern hemisphere helmet-streamer eruption in the absence of any flares.[30] The outer boundary for this study was taken at 3.6 AU so that direct comparison with Ulysses could be made. The event on April 14, 1994, was observed in real-time only by Yohkoh's soft x-ray telescope. This observation encouraged a NOAA/Space Environment Center forecaster to predict a geomagnetic storm (which occurred, with $K_p = 8$ and maximum $D_{st} = -200$ nT, where D_{st} is the geomagnetic storm disturbance index and K_p is the planetary geomagnetic index). Without the Yohkoh data, the prediction would have been for quiet conditions. Ulysses, at 3.2 AU and E 30°S 60°, observed a forward and reverse shock structure and the interplanetary evolution of a CME. By iteration of the input pressure pulse parameters, we obtained excellent timing at both Earth and at Ulysses. Our simulated data comparison with the observed data set at Ulysses is shown in Fig. 4; although some trends are indicated in the simulation, it is clear that more study is required. There were no L1 or IMP-8 spacecraft on station in the solar wind at that time. We suggest that the comparison of the left and right panels is indicative, again, of the efficacy of the deterministic three-dimensional MHD approach that should be explored further.

Finally, we provide a second example of a three-dimensional MHD study. During the maximum phase of solar cycle 22, the March 1991 period provided a series of large solar flares. Detailed summaries of the solar events, interplanetary observations, and magnetospheric consequences (including deleterious effects on near-Earth spacecraft) are given in the literature.[2,31] An effort to mimic the solar events and interplanetary consequences, via three-dimensional MHD numerical simulations, has recently been attempted by Odstrcil et al.[32] The results, described subsequently, emphasize the main problem of the numerical simulations, initialization of interplanetary disturbances as a consequence of complex solar activity and the consequences thereof as observed at different locations. The challenges faced by the space weather modeler will become starkly self-evident in the inhomogeneous, ever-changing, inner-heliospheric wind tunnel.

The period from March 16–26, 1991, was marked by 17 solar flares in several active regions on the visible solar disk, as listed in Table 1. The start, maximum, and end times (universal time) of the optical $H\alpha$ solar patrol is given after the date in Table 1. The heliolatitude and heliolongitude in a sun-centered spherical coordinate system are listed, followed by the optical and soft x-ray classifications, and NOAA active region (AR) numbers. The NOAA/USAF optical system refers to the flare sizes (where 4B is the rarely observed, largest, bright-B flare). The NOAA GOES spacecraft's full disk (integrated), soft x-ray flux (Wm^{-2}) in the 0.1 – 0.8 nm bandwidth provides the other classification. Flares are rated A, B, C, M, or X according to the peak flux intensity in that wavelength channel. A very small flare in the A class has a peak x-ray flux of $>10^{8}$ Wm^{-2}; a moderately intense flare in the C-class has a peak flux $>10^{-6}$ Wm^{-2}, etc. Flares are further subclassified by the multiplicative factor within that decade; e.g., a 1.8×10^{-4} Wm^{-2} peak flux (flare 1 in Table 1) is an X1.8 flare. However, because X is the highest classification, a rarely observed 3×10^{-3} Wm^{-2} peak flux would be classified as a X30 flare. As noted in Sec. II, the duration (1/e decay time, for example) of the flare's soft x-ray intensity rise above background may be used as a proxy for the piston-driven time of a coronal shock wave that may be detected by the USAF's radio astronomical detection system at various terrestrial longitudes.

The nonuniform, steady-state conditions in the three-dimensional inner heliosphere (from 0.1 to 2.6 AU) were estimated by starting from measured line-of-sight, photospheric magnetic fields; using a potential field calculation to provide helioradial magnetic fields at a source surface (for example, $2.5R_{\odot}$); and then empirically extrapolating this radial field (B_r) to the computational domain's lower boundary at 0.1 AU. Radial and azimuthal velocities are also empirically determined, together with an assumed meridional velocity, $V_\theta = 0$, at this boundary.

The density is chosen to keep the total pressure (sum of thermal and magnetic pressures) in equilibrium for an assumed constant temperature at the same boundary. Thus, the nonuniform, steady-state condition in the computational domain ($0.1 \leq r \leq 2.6$ AU, $30 \leq \theta \leq 150$ deg, $0 \leq \phi \leq 360$ deg, and a computational mesh $125 \times 20 \times 72$) is obtained via the time-relaxation technique. The angles θ and ϕ are the spherical coordinates in the polar and longitudinal directions, respectively. This resulting situation on March 16,

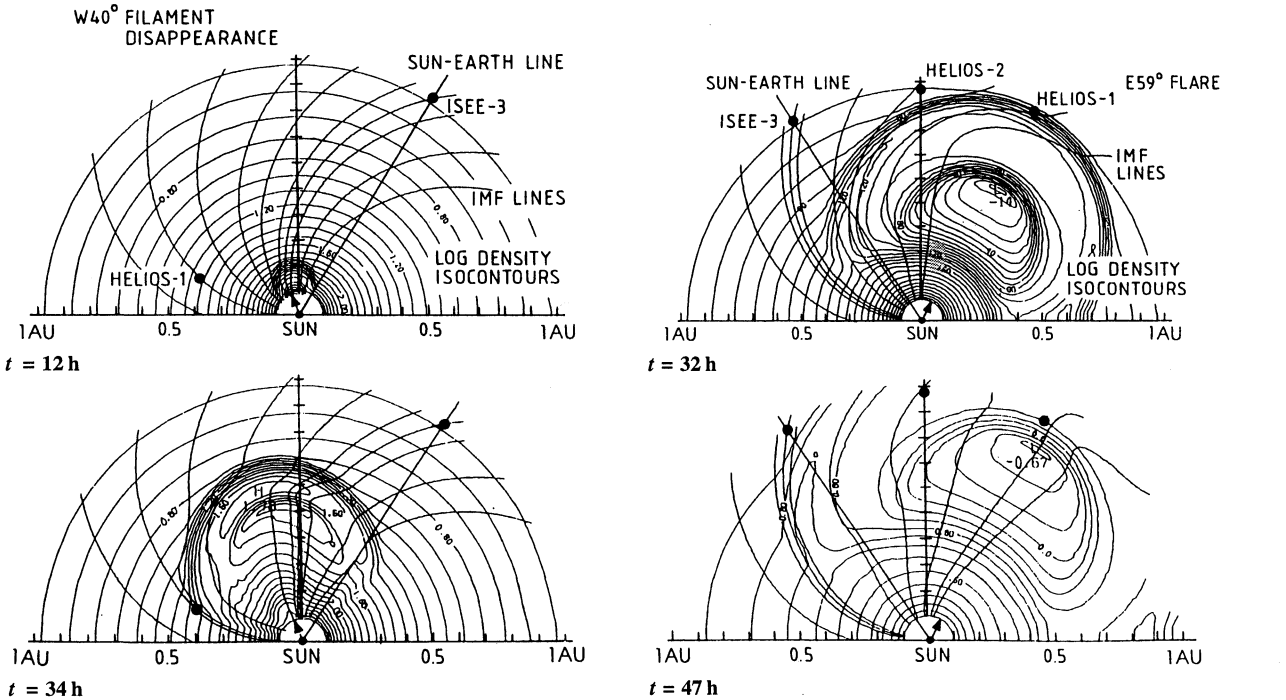

Fig. 3 Simulation of the shock propagation for: Dec. 8, 1981, west event (left panels) and Feb. 18, 1979, east events (right panels) (from Ref. 29).

Table 1 March 1991 solar flares

Date	Start	Maximum	End	Latitude,°	Longitude,°	Opt	X ray	Region
March 16, 1991	0047	0050	0109	S09	E09	2B	X1.8	6545
March 16, 1991	2144	2156	2220	S09	W04	2B	M6.0	6545
March 17, 1991	0926	0932	0953	S25	E83	2B	M2.1	6555
March 17, 1991	1435	1440	1452	S26	E93	2B	M2.3	6555
March 17, 1991	2054	2126	2305	S10	W13	2B	X1.0	6545
March 18, 1991	2303	2307	0017	S10	W34	2B	M1.3	6545
March 19, 1991	0147	0158	0240	S10	W33	2B	M6.7	6545
March 21, 1991	0036	0050	0110	S23	E51	2B	M1.5	6555
March 21, 1991	1029	1041	1051	S24	E48	2B	M2.6	6555
March 21, 1991	2337	2343	0126	S25	E40	2B	M5.4	6555
March 22, 1991	2243	2245	2317	S26	E28	3B	X9.4	6555
March 23, 1991	0305	0510	0623	S24	E11	2B	M6.8	6555
March 23, 1991	2202	2222	2249	S23	E06	2B	M5.6	6555
March 24, 1991	0239	0244	0421	S15	E51	2B	M3.2	6558
March 25, 1991	0008	0022	0100	S24	W08	3B	X1.1	6555
March 25, 1991	0758	0818	0844	S24	W13	3B	X5.3	6555
March 26, 1991	2026	2034	2137	S28	W23	3B	X4.7	6555

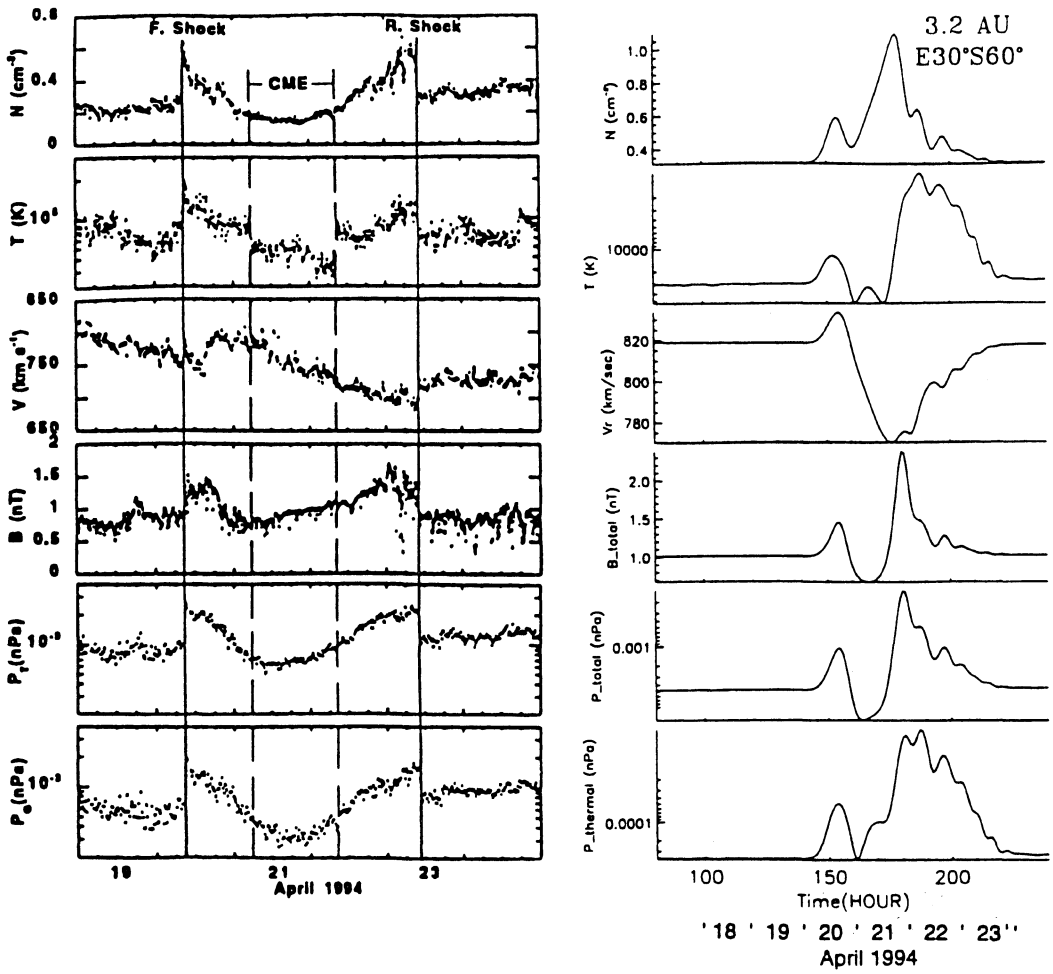

Fig. 4 Comparison of Ulysses observations (3.2 AU; S 60°, E 30°) in the left-hand column with three-dimensional MHD simulation in the right-hand column during the April 19–23, 1994, events. The simulation at Earth is not shown because no spacecraft observations were made at this time period (from Ref. 30).

1991, is then used as the initial condition for the simulation of transient disturbances.

The interplanetary disturbances are initialized at the appropriate times in Table 1, by increase of the velocity, duration, and width. It is well known that no observations are available to provide these input conditions. The proxy soft x-ray duration, $H\alpha$ optical flare location, and white light statistical widths of CMEs are then used as ad hoc approximations because no alternatives are provided in the literature for this use of the classical initial boundary-value problem. Thus, the input pulse velocity and spatial diameter are provided by an ad hoc flare importance conversion table.[32,33] The pulse start time, in each case, is delayed by the time required for the pulse to propagate to 0.1 AU with its initial velocity.

Figure 5 shows the distribution of total density contours in the ecliptic plane. The nonuniform steady-state at 0 h on March 16, 1991 (upper left), shows the two traces of the warped heliospheric current/heliospheric plasma sheet (HCS/HPS) where it penetrates the ecliptic plane as a result of the corotating interaction regions. Six flares have already taken place by the time of the next view three days later (upper right). The letters on these plots, moving away from the sun, represent the locations of Mercury, Venus, Earth (on a 1-AU circle), Galileo, Mars, and Ulysses, respectively.

The complexity of the interactions with each other and their distortion of the HCS/HPS (followed by the eventual recovery of the corotating shape of the latter following termination of the disturbances) is self-evident. Despite this complexity, one can gain some

insight to the interactions that may actually have taken place during the simulated time of March 16–31, 1991. The obvious question arises: How real is this simulation? Were any of the flares in Table 1 ineffective (for some unknown reason) in generating interplanetary consequenes?

Thus, a secondary, more conservative, approach was adopted to investigate this question. Four of the flares, listed in Table 2, were associated with type II radio drifts, which, when converted to coronal shock velocities, provided magnetic Rankine–Hugoniot jump conditions for input pulse parameters. The rest of the flares were, in effect, neglected. The start time of the type II burst, its maximum strength at the listed flare position, the measured shock velocity, its assumed radius over which this strength was taken to decay sinusoidally, and the flare's x-ray duration as a proxy for piston-driven shock motion prior to its blast-wave motion are given in Table 2.

Figure 6 shows the temporal evolution (March 16–31, 1991) of the solar wind's radial velocity V_r at the Earth (Imp-8), Ulysses, Pioneer Venus-Orbiter, and Galileo in the panels, respectively, from top to bottom. The solid line is the result from the earlier, 17-flare simulation, the dashed line is from the secondary more conservative approach just outlined. The superimposed observational data are from NASA's National Space Science Data Center. The large data

Table 2 Selected March 1991 shock and pulse parameters

Date	Start	Position	Shock velocity, km/s	Radius, deg	Duration, h:min
March 17	14:35	S26 E93	1425	45	01:00
March 19	01:23	S09 W32	1750	45	00:30
March 22	22:47	S26 E28	4000	45	01:23
March 23	01:49	S24 E05	1300	45	06:00

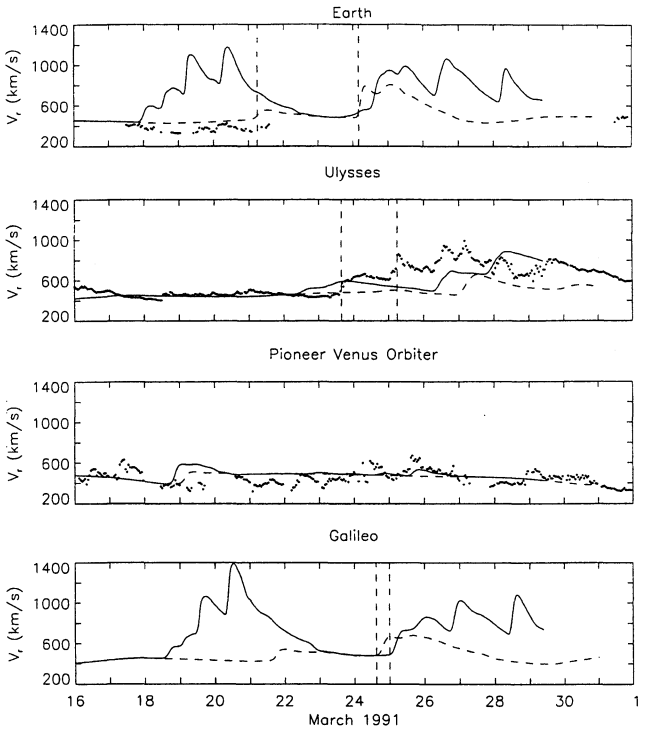

Fig. 6 Comparison of the three-dimensional MHD simulated radial solar wind velocity, as computed by two separate initialization procedures, with observational data (from Ref. 32).

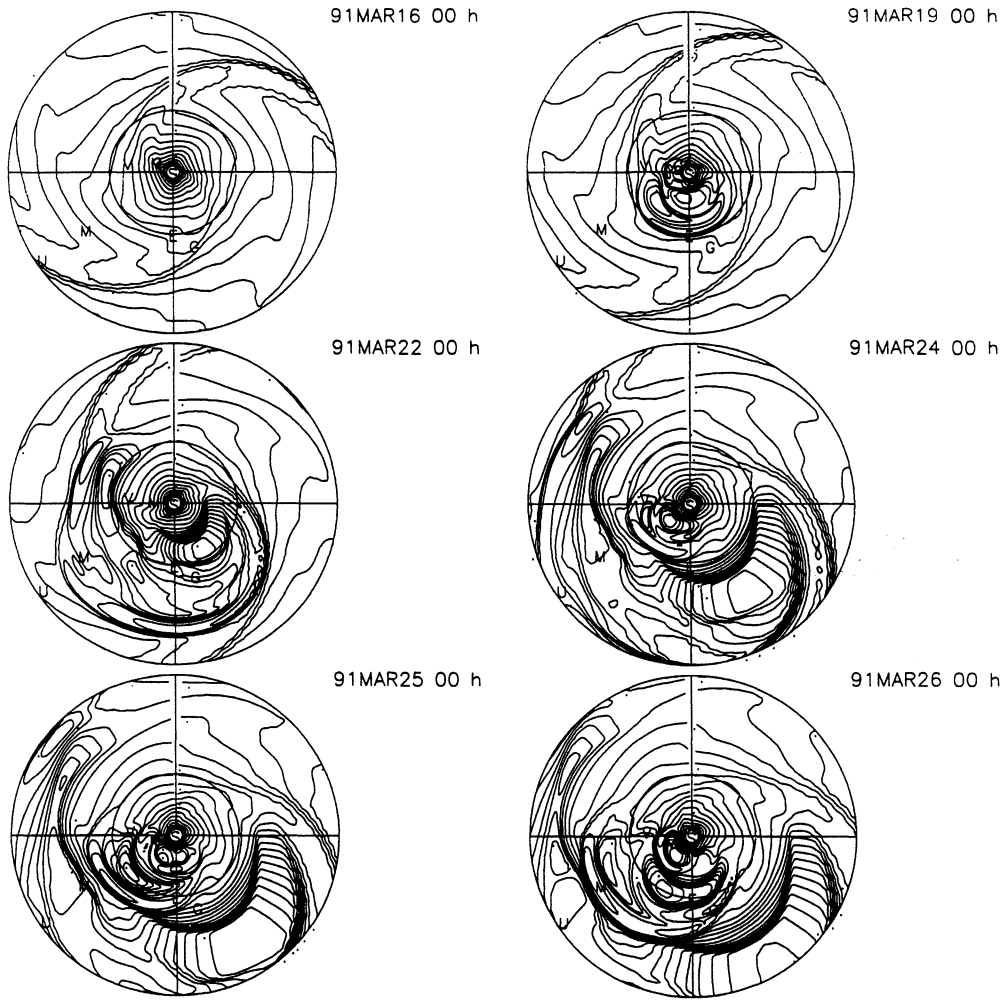

Fig. 5 Contours of solar wind density and interplanetary plasma clouds in the ecliptic plane for the 17 flares during March 16–26, 1991, from the three-dimensional MHD simulation of Odstrcil et al.[32]

gap at Earth was due to the Imp-8 immersion at that time in the magnetospheric tail. Galileo did not obtain any plasma data during its cruise phase to Jupiter; however, limited magnetometer data detected two shocks as shown by the two vertical dashed lines in the bottom panel. Two storm sudden commencements indicate shock arrivals at Earth (vertical dashed lines). Also, two shock arrivals are similarly indicated at Ulysses.

It might be suggested that the second approach was more successful than the first one, for this particular parameter V_r, because of the good shock agreements at Earth. This suggestion is premature because space here precludes comparison of other important physical parameters such as density and B_θ (the latter being important since it is equal to $-B_z$, the essential parameter required for geomagnetic storm forecasts). A detailed study of this kind has not been done.

The important point to be emphasized here is this: No procedure has ever been done on a scale such as this one. We suggest that this wind tunnel approach is a necessary first step in the direction of validation studies. The difficulties in choosing initialization conditions and obtaining multiple, continuous data acquisition for checking simulations cannot be overemphasized.

Concluding Remarks

A brief review was given of the application of classical hypersonic gasdynamics and MHD to some problems in space plasma physics. Reference was made to extensive reviews of one-, two-, and three-dimensional MHD applications. Several examples in the two-dimensional MHD category, i.e., in the ecliptic plane, and two examples in three-dimensional MHD were given. We do not believe that there is any alternative to the validation procedure proposed by the three-dimensional MHD cases if both scientific and operational objectives are to be pursued. Despite the simplifying assumptions (ideal, one fluid, with an adiabatic exponent of $\frac{5}{3}$) and access to limited solar observations for specification of initialization physical parameters, we suggest that three-dimensional MHD can provide a powerful tool for eventual modular insertion into a seamless, sun–Earth, space weather forecasting system.

Acknowledgments

The author wishes to thank the three referees for their useful and constructive suggestions.

References

[1]"National Space Weather Program Strategic Plan," Office of the Federal Coordinator for Meteorological Services and Supporting Research, Silver Spring, MD, 1995; also National Space Weather Program Implementation Plan, FCM-P31-1997, Jan. 1997.

[2]Allen, J. H., and Wilkinson, D. C., "Solar-Terrestrial Activity Affecting Systems in Space and on Earth," *Solar-Terrestrial Predictions-IV*, edited by J. Hruska, M. A. Shea, D. F. Smart, and G. Heckman, Vol. 1, National Oceanic and Atmospheric Administration/Environmental Research Labs., Dept. of Commerce, Boulder, CO, 1993, pp. 75–107.

[3]Inouye, M., and Lomax, H., "Comparison of Experimental and Numerical Results for the Flow of a Perfect Gas About Blunt Bodies," NASA TN D-1426, 1962.

[4]Dryer, M., and Faye-Petersen, R., "A Gasdynamic Analog for the Solar Wind Flow Around an Assumed Magnetospheric Boundary," *Transactions, American Geophysical Union*, Vol. 45, Dec. 1964, p. 630.

[5]Dryer, M., and Faye-Petersen, R., "Magnetogasdynamic Boundary Condition for a Self-Consistent Solution to the Closed Magnetopause," *AIAA Journal*, Vol. 4, No. 2, 1996, pp. 246–254; also AIAA Paper 65-121, Jan. 1965.

[6]Dryer, M., and Heckman, G. R., "On the Hypersonic Analogue as Applied to Planetary Interaction with the Solar Plasma," *Planetary Space Science*, Vol. 15, April 1967, pp. 515–546.

[7]Dryer, M., and Heckman, G. R., "Application of the Hypersonic Analog to the Standing Shock of Mars," *Solar Physics*, Vol. 2, March 1967, pp. 112–124.

[8]Dryer, M., Rizzi, A. W., and Shen, W.-W., "Interaction of the Solar Wind with the Outer Planets," *Astrophysics and Space Science*, Vol. 22, No. 2, 1972, pp. 329–351.

[9]Spreiter, J. R., and Alksne, A. Y., "Solar-Wind Flow Past Objects in the Solar System," *Annual Review of Fluid Mechanics*, Vol. 2, 1970, pp. 313–354.

[10]Sedov, L. I., *Similarity and Dimensional Methods in Mechanics* (English translation by M. Holt and M. Friedman), 4th ed., Academic, New York, 1959, Chaps. 4 and 5.

[11]Korobeinikov, V. P., "Gas Dynamics of Explosions," *Annual Review of Fluid Mechanics*, Vol. 3, 1971, pp. 317–346.

[12]Belotserkovskii, S. M., "Study of the Unsteady Aerodynamics of Lifting Surfaces Using the Computer," *Annual Review of Fluid Mechanics*, Vol. 9, 1977, pp. 469–494.

[13]Dryer, M., and Jones, D. L., "Energy Deposition in the Solar Wind by Flare-Generated Shock Waves," *Journal of Geophysical Research*, Vol. 73, No. 15, 1968, pp. 4875–4881.

[14]Dryer, M., "Interplanetary Shock Waves Generated by Solar Flares," *Space Science Reviews*, Vol. 15, No. 4, 1974, pp. 403–468.

[15]Dryer, M., "Interplanetary Shock Waves: Recent Developments," *Space Science Reviews*, Vol. 17, Nos. 2–4, 1975, pp. 277–325.

[16]Dryer, M., "Coronal Transient Phenomena," *Space Science Reviews*, Vol. 33, Nos. 1, 2, 1982, pp. 233–275.

[17]Dryer, M., "Interplanetary Studies: Propagation of Disturbances Between the Sun and the Magnetosphere," *Space Science Reviews*, Vol. 67, Nos. 3, 4, 1994, pp. 363–419.

[18]Dryer, M., and Smart, D. F., "Dynamical Models of Coronal Transients and Interplanetary Disturbances," *Advances in Space Research*, Vol. 4, No. 7, 1984, pp. 291–301.

[19]Smart, D. F., Shea, M. A., Dryer, M., Quintana, A., Gentile, L. C., and Bathurst, A. A., "Estimating the Arrival Time of Solar-Flare-Initiated Shocks by Considering Them to Be Blast Waves Riding over the Solar Wind," *Solar-Terrestrial Predictions*, edited by P. A. Simon, G. Heckman, and M. A. Shea, National Oceanic and Atmospheric Administration, Dept. of Commerce, and Air Force Geophysics Lab., Dept. of Defense, Boulder, CO, 1986, pp. 471–481.

[20]Smith, Z. K., and Dryer, M., "The Interplanetary Shock Propagation Model: A Model for Predicting Solar-Flare-Caused, Geomagnetic Sudden Impulses Based on the $2\frac{1}{2}$D, MHD Numerical Simulation Results from the Interplanetary Global Model (2D IGM)," National Oceanic and Atmospheric Administration Tech. Memo Environmental Research Labs./Space Environment Lab., ERL/SEL-89, July 1995.

[21]Nakagawa, Y., Hu, Y. Q., and Wu, S. T., "The Method of Projected Characteristics for the Evolution of Magnetic Arches," *Astronomy and Astrophysics*, Vol. 179, April 1987, pp. 354–370.

[22]Hu, Y. Q., and Wu, S. T., "A Full-Implicit-Continuous-Eulerian (FICE) Scheme for Multidimensional Transient Magnetohydrodynamic (MHD) Flows," *Journal of Computational Physics*, Vol. 55, No. 1, 1984, pp. 33–64.

[23]Wu, S. T., and Wang, J. F., "Numerical Tests of a Modified Full Implicit Continuous Eulerian (FICE) Scheme with Projected Normal Characteristic Boundary Conditions for MHD Flows," *Computational Methods in Applied Mechanics and Engineering*, Vol. 64, Nos. 1–3, 1987, pp. 267–282.

[24]Sun, M. T., Wu, S. T., and Dryer, M., "On the Time-Dependent Numerical Boundary Conditions of Magnetohydrodynamic Flows," *Journal of Computational Physics*, Vol. 116, March 1995, pp. 330–342.

[25]Wu, S. T., Guo, W. P., and Wang, J. F., "Dynamical Evolution of a Coronal Streamer-Bubble System," *Solar Physics*, Vol. 157, Nos. 1, 2, 1995, pp. 325–348.

[26]Wu, S. T., Guo, W. P., Dryer, M., Tsurutani, B. T., and Vaisberg, O. L., "Evolution of Coronal MHD Shocks," *Proceedings of First US–Russian Scientific Workshop on the FIRE Mission's Space Environment*, edited by O. L. Vaisberg and B. T. Tsurutani, Space Research Inst. (IKI), Moscow, 1995, pp. 266–272.

[27]Smith, Z., and Dryer, M., "Numerical Simulations of High Speed Solar Wind Streams Within 1 AU and Their Signatures at 1 AU," *Solar Physics*, Vol. 131, No. 2, 1991, pp. 363–383.

[28]Dryer, M., Smith, Z. K., Coates, A. J., and Johnstone, A. D., "The February 1986 Solar Activity: A Comparison of Giotto, Vega-1, and Imp-8 Solar Wind Measurements With MHD Simulations," *Solar Physics*, Vol. 132, No. 2, 1991, pp. 353–371.

[29]Heras, A. M., Sanahuja, B., Lario, D., Smith, Z. K., Detman, T., and Dryer, M., "Three Low-Energy Particle Events: Influence of the Parent Interplanetary Shock," *Astrophysical Journal*, Vol. 445, May 20, 1995, pp. 497–508.

[30]Dryer, M., Wu, C.-C., and Smith, Z. K., "3D MHD Simulation of the 14 April 1994 'ICME' and its Propagation to Earth and Ulysses," *Journal of Geophysical Research*, Vol. 102, No. A7, 1997, pp. 14065–14074.

[31]Shea, M. A., Smart, D. F., Watanabe, T., Sanahuja, B., and Flueckiger, E. O., "Summary of Solar, Interplanetary, and Geomagnetic Disturbances During SOLTIP Interval 1 (22–27 March 1991)," *Proceedings of the Second SOLTIP Symposium*, edited by T. Watanabe, Ibaraki Univ., Nakaminato, Japan, *STEP GBRSC News*, Vol. 5, Special Issue, 1995, pp. 13–22.

[32]Odstrcil, D., Dryer, M., and Smith, Z., "Numerical Simulation of March 1991 Interplanetary Disturbances (SOLTIP Interval 1)," *Proceedings of the Third SOLTIP Symposium*, edited by X.-S. Feng, Pergamon, Beijing, PRC (to be published).

[33]Akasofu, S.-I., and Fry, C. D., "A First Generation Numerical Geomagnetic Storm Prediction Scheme," *Planetary Space Sciences*, Vol. 34, Jan. 1986, pp. 77–92.

G. M. Faeth
Associate Editor